

The potential of plant biomarker evidence derived from rock hyrax middens as an indicator of palaeoenvironmental change

Andrew S. Carr^{a,*}, Arnoud Boom^a, Brian M. Chase^b

^a Department of Geography, University of Leicester, LE1 7RH, UK

^b Institute for Human Evolution, University of the Witwatersrand, Wits 2050, South Africa

ARTICLE INFO

Article history:

Received 15 July 2009

Received in revised form 16 November 2009

Accepted 22 November 2009

Available online 30 November 2009

Keywords:

Procavia

Quaternary

South Africa

Lipids

Stable isotopes

ABSTRACT

Hyrax middens are unique environmental archives with the potential to provide unprecedented high-resolution palaeoenvironmental records, particularly in the arid regions of southern Africa. This study provides the first detailed characterisation of the organic matter composition of hyraceum and aims to identify biomarker evidence capable of providing new or supplementary palaeoenvironmental data from these novel archives. Pyrolysis gas chromatography mass spectrometry reveals hyraceum to be dominated by nitrogen-containing aromatic compounds, notably benzamide. This is almost certainly derived directly from the hyrax urine and is probably the main source of nitrogen as measured in bulk $\delta^{15}\text{N}$ measurements. Solvent-extractable lipids comprise homologous suites of long-chain *n*-alkanes (C_{24} – C_{34}) and *n*-alkanols (C_{16} – C_{26}), characteristic of higher plant leaf waxes, along with an abundance of animal-derived sterols, higher plant sterols and terpenoids; as well as the ubiquitous benzamide.

n-alkane distributions and compound specific $\delta^{13}\text{C}$ clearly differentiate samples from the C_3 vegetation dominated Cape Floristic Region, and the more arid, C_4 grass-rich savannas of central Namibia (Klein Spitzkoppe). Distinct changes in *n*-alkane distribution and $\delta^{13}\text{C}$ are observed within the Spitzkoppe midden; most notably the mid to late Holocene period (c. 6000–2000 cal yr BP), which records a progressive reduction in grass-derived organic matter inputs. Based on the animal's feeding behaviour and contemporary site ecology, a phase of increasing aridity is inferred, which is consistent with other proxy data from this site (e.g. bulk $\delta^{15}\text{N}$). The excellent preservation of plant and animal biomarkers suggests that there is significant potential for midden-derived biomarkers to provide long-term palaeoenvironmental proxies.

Crown Copyright © 2009 Published by Elsevier B.V. All rights reserved.

1. Introduction

The rock hyrax (Procaviidae: *Procavia capensis*) is a medium sized gregarious herbivore common throughout Africa. Colonies of this species have a habit of defecating and urinating in the same location, resulting in the progressive accumulation of 'middens' composed of a yellow-brown compact material known as hyraceum. In arid environments hyraceum has a high preservation potential within the rock overhangs and crevices the animal inhabits and can form stratified deposits many tens of centimetres thick. In the drylands of southern Africa palaeoecological archives of significant length and/or resolution are extremely rare (Chase and Meadows, 2007). The recognition that hyraceum deposits may be of considerable (Pleistocene) antiquity, and that they preserve palaeoecological proxies such as pollen (Scott and Bousman, 1990; Scott, 1996) has generated considerable interest

(Scott et al., 2004; Gil-Romera et al., 2006a,b; Scott and Woodborne, 2007; Meadows et al., in press). The more recent demonstration that hyraceum preserves records of near-decadal resolution (Chase et al., 2009) serves to underline the great potential of these archives.

Hyraxes are not thought to feed much further than c. 60–500 m from the rock overhangs/koppies they inhabit and are relatively unselective feeders, suggesting that their diet and associated faeces reflect contemporary local vegetation (Sale, 1965; Hoeck, 1975; Brown and Downs, 2005). Many studies have therefore utilised palynological evidence within hyraceum to reconstruct local palaeovegetation (e.g. Scott and Bousman, 1990; Gil-Romera et al., 2006a,b). There is also an increasing emphasis on the potential of stable isotope records obtained from midden material (Scott and Vogel, 2000; Chase et al., 2009). Analysis of $\delta^{13}\text{C}$ of organic matter is particularly pertinent in this region as southern African vegetation is characterised by plants exhibiting all three major photosynthetic pathways (C_3 , C_4 and CAM), with their distribution closely related to the region's climate. C_3 vegetation dominates in the winter-rainfall affected Cape Floristic Region (Vogel et al., 1978; Fig. 1), while the sub-tropical summer-rainfall environments covering the greater part of the sub-continent are characterised by a significant proportion of C_4 vegetation. Organic matter derived from

* Corresponding author. Tel.: +44 0 116 2523851.

E-mail address: asc18@le.ac.uk (A.S. Carr).

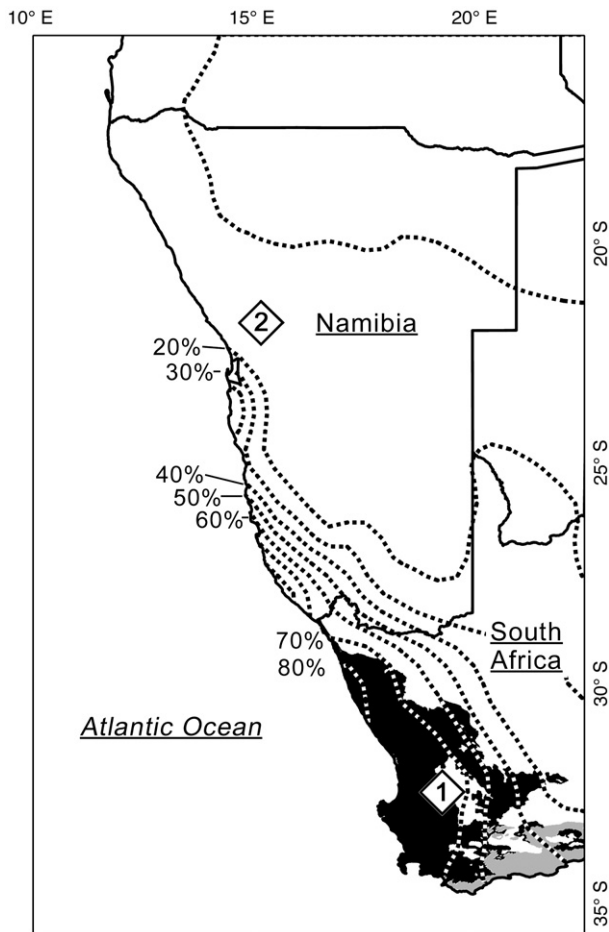


Fig. 1. Southern African rainfall seasonality indicated as percentage of annual precipitation falling in April–September. This distinct seasonality patterning reflects the position of the sub-continent at the margins of the sub-tropical climate system, such that rain-bearing westerly systems cross the Western Cape throughout the winter months. C₃ (black) and C₄ (white) plant and mixed C₃/C₄ (grey) distributions are shown along with the sample site locations; Truitjes Kraal (1) Klein Spitzkoppe (2).

the C₃ and C₄ photosynthetic pathways displays distinct isotopic signatures, reflecting their differing discrimination against ¹³C during photosynthesis (Farquhar et al., 1989). CAM plant ¹³C values are highly variable, but generally lie between those of C₃ and C₄ plants. This is because some species exhibit C₃/CAM flexibility, while others may be obligate CAM plants (Rundel et al., 1999). In southern Africa they are particularly prevalent in the Succulent and Nama Karoo Biomes (Cowling and Hilton-Taylor, 1999).

It is well established that herbivore faecal matter reflects the ¹³C of the vegetation consumed by the animal (e.g. Codron et al., 2007 and references therein). More recently Chase et al. (2009) suggested a strong linkage between (plant-derived) ¹⁵N signals in hyraceum and environmental moisture availability. Hyrax middens essentially comprise varying proportions of faecal pellets and concentrated urine, as well as additional–potentially allochthonous–material such as hair, aeolian dust, plant fragments and pollen (Scott, 1996; Scott and Woodborne, 2007). In hot and dry conditions the urine rapidly evaporates, precipitating salts (primarily KCl with smaller amounts of the carbonate minerals vaterite and weddellite; Scott and Woodborne, 2007; Prinsloo 2007), which seal in much of the associated organic matter. The inorganic composition of hyraceum was recently reported (Prinsloo, 2007), but the associated organic matter has yet to be considered in any detail. A range of important insights can be obtained from the analysis of coprolitic organic matter, particularly from the

specific organic compounds indicative of living organisms (biomarkers) that may be preserved (e.g. Hollocher et al., 2001). Coprolite studies utilising plant and animal biomarkers have previously considered palaeo-dietary reconstructions in archaeological research (e.g. Lin and Conner, 2001), and palaeo-diet/palaeoecological reconstructions for now-extinct fauna (van Geel et al., 2008). The latter study demonstrated the clear preservation of plant biomarkers, specifically leaf wax lipids, within herbivore digestive tracts.

Many plant biomarker palaeoenvironmental studies have specifically employed leaf wax lipids (e.g. *n*-alkanes, *n*-alkanols; *n*-alkanoic acids; Collister et al., 1994), which may be widely distributed in the environment and are diagnostic of differing plant sources (Conte and Weber, 2002). In southern Africa Rommerskirchen et al. (2003) analysed leaf waxes within Late Holocene (terrestrially-derived) marine sediments in the southeast Atlantic Ocean. They demonstrated that the relative abundances of *n*-alkane and *n*-alkanol homologues, along with compound specific stable carbon isotope signals, tracked large-scale ecological patterns on the African continent, particularly the distribution of tropical C₃ vegetation and C₄ grass-rich savanna ecosystems. Schefuß et al. (2003) reported comparable patterns for North Africa, while studies elsewhere have also related lipid distributions to changes in humidity and/or aridity (e.g. Castañeda et al., 2009). A clear implication of these studies is that palaeoecological and palaeoclimatic fluctuations can be recorded in archives preserving leaf wax lipids (e.g. Rommerskirchen et al., 2006). Hyraceum deposits therefore offer a unique opportunity to systematically develop this approach in a region where suitable archives are usually lacking.

Given their relatively recalcitrant nature leaf wax lipids should survive transit through the Hyrax's digestive tract and be subsequently preserved within hyraceum. Furthermore, unlike ¹³C isotope analyses of total organic matter, individual leaf waxes ¹³C signals can provide a direct and unequivocal insight into an animal's past dietary habits, which are in turn related to changes in the local environment (see references above). An additional advantage of this approach is that leaf wax homologue distributions can also be obtained relatively rapidly from total solvent extracts, and may provide a means for the rapid identification of major palaeoecological shifts within long hyraceum sequences. The overall aim of this paper therefore is to provide an initial assessment of the organic matter composition and lipid biomarker suites preserved within hyraceum, with particular emphasis on assessing the potential of solvent-extractable leaf wax lipids as a palaeoenvironmental proxy. In conjunction, we consider the (insoluble) macromolecular organic matter composition of the hyraceum. As solvent-extractable lipids typically comprise a small percentage of the total organic matter in a sample, the analysis of macromolecular organic matter provides a means to assess the major sources of carbon and nitrogen as determined in total organic carbon (TOC) and total nitrogen (TN) stable isotope analyses (e.g. Scott and Vogel, 2000; Chase et al., 2009). The macromolecular organic matter fraction will likely comprise high molecular weight and/or polymeric organic compounds (a typical plant-derived example is lignin), but to date this has never been investigated with hyraceum (c.f. Hollocher et al., 2001).

The overall aims of the study are:

1. To characterise the major solvent-extractable and macromolecular constituents of hyraceum organic matter and to assess organic matter provenance and preservation.
2. To assess the potential of leaf wax lipids and compound specific *n*-alkane ¹³C analyses as palaeoenvironmental proxies using a long (c. 12,000 year) hyraceum sequence for which additional proxy data are presently available.
3. Consider the results of 1 and 2 in light of sample site ecology, and assess the wider implications for reconstructing terrestrial palaeoecological change in southern Africa using this approach.

2. Sample details

In this study we selected two midden sites representative of distinct biomes and climatic settings within southern Africa. The first site (Truitjes Kraal; henceforth “TK”) is in the southern Cederberg Mountains of the Western Cape Province of South Africa at an altitude of c. 890 m (Fig. 1). This region is characterised by sclerophyllous, shrubby “fynbos” vegetation of the Cape Floristic Region (e.g. Linder, 2003). This vegetation consists primarily of C₃ plants, including grasses such as *Pentstemonis* sp. from the C₃ Pooideae sub-family (Gibbs-Russell et al., 1990). C₄ grasses are not typically found in the Cederberg (Vogel et al., 1978). Some small trees are present, (e.g. *Searsia undulata*; formerly *Rhus undulata*), and the site lies within a few kilometres of the ecotone between the Fynbos and the Succulent Karoo Biomes (Meadows et al., in press). The latter region is relatively rich in succulent (frequently CAM) species, and a number of succulents are also found in the vicinity of the sample site; notably species from the Crassulaceae and Mesembryanthemaceae families (Meadows et al., in press). The climate in this region is dominated by winter-rainfall and at the TK site mean annual rainfall is currently c. 250 mm a⁻¹ (Schulze, 1997). The TK midden ranges in age from 9510 to 1310 cal yr BP (Meadows et al., in press). In this study representative material from a sub-sample dating to 7000–8000 cal yr BP was analysed (Fig. 2). Palynological analyses suggest comparable vegetation to the present at this time (ibid).

The second midden investigated was obtained from the Namibian inselberg Klein Spitzkoppe (henceforth referred to as “SP”), approximately 140 km northeast of Walvis Bay (21°49'S, 15°11'E). The site lies between the Namib Desert in the west and the highland plateau of central Namibia to the east. Presently the site receives c. 135 mm of rainfall per annum, the majority of which (>70%) falls in the summer months January–March (Hijmans et al., 2005). Modern vegetation comprises very dry savanna (specifically, Xeric Namibian savanna woodland; Barnard, 1998), which includes *Sterculia* sp., Euphorbiaceae, Asteraceae, Scrophulariaceae and Capparceae (Gil-Romera et al., 2006b). Grasses are primarily C₄ type and belong to the sub-families Chloridoideae and Arundinoideae (e.g. *Stipagrostis* sp.); Gibbs-Russell et al., 1990; Schulze et al., 1996; Gil-Romera et al., 2006b). The inselberg does however receive more rain than the surrounding lowlands, and more mesic vegetation is present on the lower-most slopes (e.g. Oleaceae, Vitaceae). Radiocarbon dating indicates that the SP midden covers the period from c. 11,700 cal yr BP to the present (Chase et al., 2009). We have analysed a sub-section of the midden (SPZ1-3) which

dates to between 11,600 cal yr BP and 1300 cal yr BP, with an estimated accumulation rate of approximately 10.2 μm yr⁻¹ (Chase et al., 2009). This piece was further sub-sampled over its depth range of c. 150 mm (Fig. 2).

3. Methods

All samples were drilled from pieces of hyraceum, freeze-dried and homogenised in a ball-mill. Bulk elemental and stable isotope ratios were obtained using a SerCon ANCA GSL elemental analyser connected to a SerCon Hydra 20–20 continuous flow isotope ratio mass spectrometer. In the case of samples from the SP midden, which was found to contain c. 6–8% carbonate, total organic carbon (TOC) was determined after pre-treatment with dilute hydrochloric acid. All reported data are means of triplicate analyses of sub-samples. Carbon isotopic composition is reported in per mill (‰) relative to the Pee Dee Belemite (PDB) following:

$$\delta^{13}\text{C} = \left[\left(\frac{R_{\text{sample}}}{R_{\text{PDB}}} \right) - 1 \right] * 1000 (\text{‰})$$

Where $R = {}^{13}\text{C}/{}^{12}\text{C}$.

Lipid biomarkers were extracted using solvents of progressively decreasing polarity (MeOH; dichloromethane (DCM); hexane) in conjunction with ultra-sonic agitation. Extracts were pooled, evaporated with a rotary evaporator and eluted over an Al₂O₃ column to derive apolar (hexane) and polar (DCM) fractions. The polar fraction was derivatized using bis(trimethylsilyl)trifluoroacetamide (BSTFA) for 1 h at 60 °C prior to analysis.

Three additional larger samples were obtained from the top and bottom of SP and top of TK samples (Fig. 2). These were spiked with two internal laboratory standards (C₁₈ n-alkane and C₁₉ fatty acid methyl ester) in order to quantify the concentration of extracted biomarkers. Gas chromatography mass spectrometry was carried out on all samples using a Perkin Elmer Clarus 500 GC/MS system fitted with a CP-Sil 5CB MS column (30 m × 0.25 mm). The temperature programme comprised an initial temperature of 60 °C for 1 min, increased to 120 °C at a rate of 20 °C s⁻¹, then ramped to a final temperature of 310 °C at 4 °C min⁻¹. The temperature was held at 310 °C for a further 15 min of analysis. Compounds were identified on the basis of their retention times and mass spectra. Relative concentrations were based on total ion current (TIC) chromatogram peak integration using the Turbo-Mass software. Isotope ratio

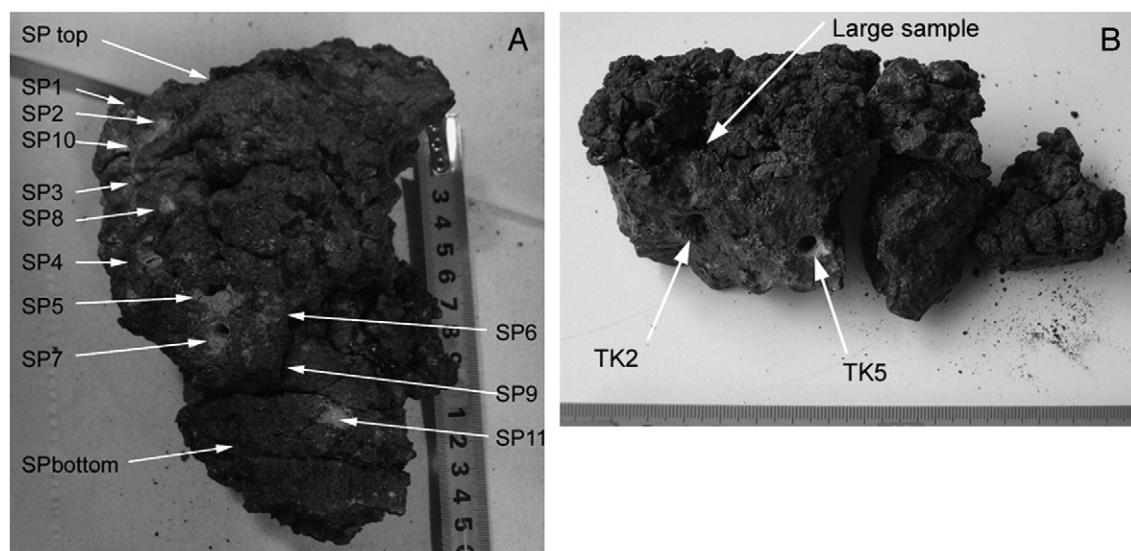


Fig. 2. The sampled material, with sub-sample locations. Both the SP midden (A) and TK midden (B) are shown.

monitoring GC/MS (irm-GC/MS) analyses were carried out using an Agilent 6890 N gas chromatograph equipped with a platinum–copper wire combustion reactor, which was interfaced to a SerCon GC-CP and connected to the Hydra 20–20 MS.

In order to characterise the insoluble macromolecular organic matter within hyraceum, we conducted pyrolysis GC/MS (py-GC/MS) analyses on these samples. A representative sample from each midden was analysed using a CDS 1000 pyroprobe coupled to a Perkin Elmer Clarus 500 GC/MS system (configured for splitless injection). Approximately 0.5 mg of freeze-dried and homogenised sample was encapsulated in a clean quartz tube (held in place with quartz wool) and was pyrolysed at 610 °C for 15 s. Samples were analysed with and without the application of an online methylating agent, tetramethyl ammonium hydroxide (TMAH). The resulting methylation prevents the complete thermal degradation of some compounds and can assist in the identification of

the likely macromolecular components in a sample. The GC settings and column type were the same as those used for the lipid analyses. The temperature programme comprised an initial temperature of 40 °C held for 1.8 minutes, which was then ramped to a final temperature of 310 °C at 4 °C min⁻¹. The temperature was then held at 310 °C for a further 20 minutes of analysis time.

4. Results

4.1. Apolar solvent-extractable compounds

The apolar fraction is dominated by peaks derived from *n*-alkane homologues with chain lengths between C₂₃ and C₃₄ (C₃₄ not always identified). Additional, but much smaller peaks with comparable retention times comprise methyl-alkanes. The absolute concentration of

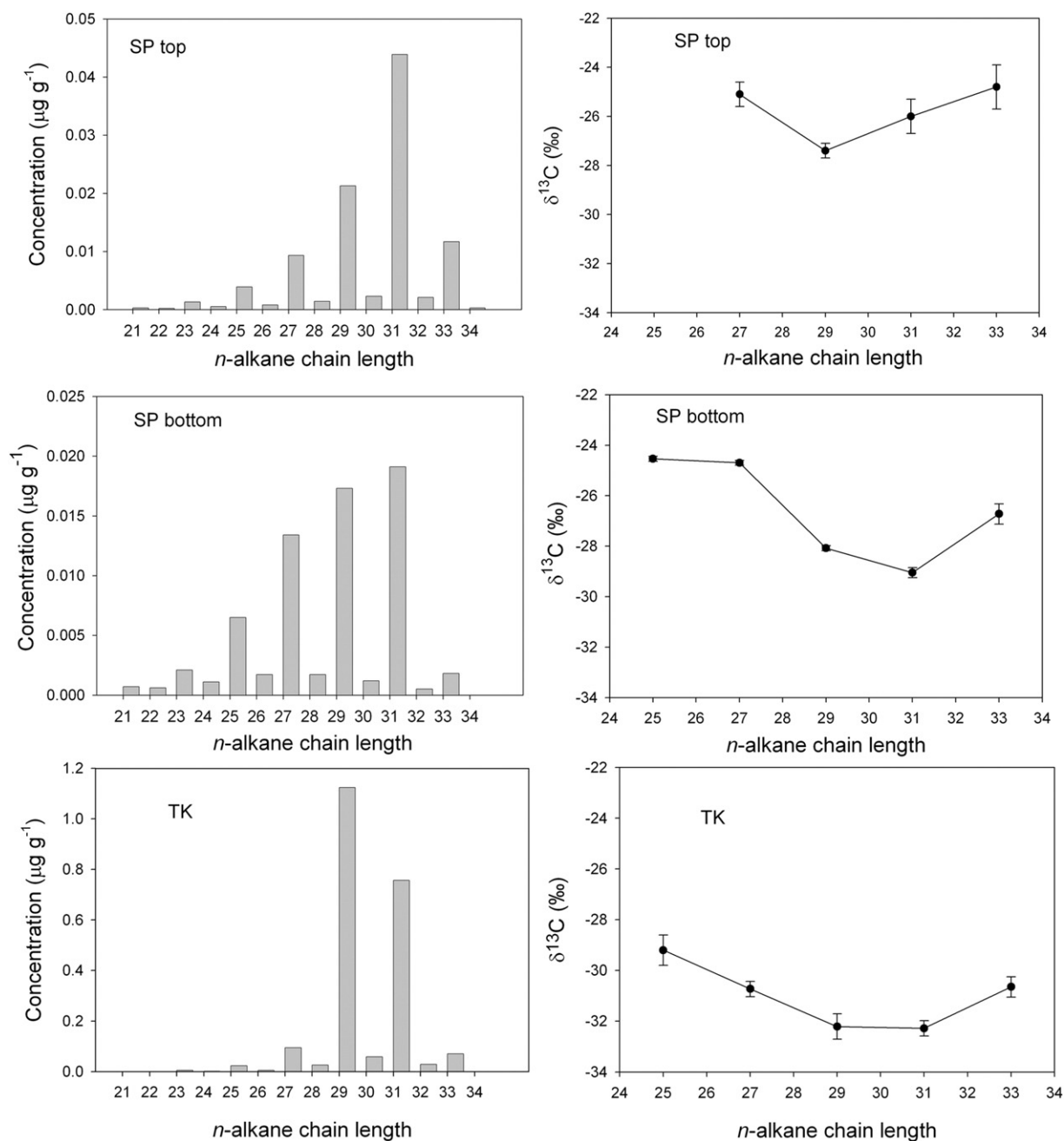


Fig. 3. *n*-alkane homologue distributions (presented as absolute concentrations) for the samples SP-top, SP-bottom and the TK midden (large sample). The mean δ¹³C values and standard deviations for the individual *n*-alkanes.

C₂₄–C₃₃ *n*-alkanes (Fig. 3) is low when compared, for example, to ocean cores (0.4–0.7 $\mu\text{g g}^{-1}$; Huang et al., 2000) or some terrestrial sedimentary contexts (0.5–1.3 $\mu\text{g g}^{-1}$ Zhang et al., 2006). The concentrations at Spitzkoppe range from <0.001 to 0.05 $\mu\text{g g}^{-1}$, but are significantly higher in the TK sample (up to 1.12 $\mu\text{g g}^{-1}$), which is commensurate with the bulk TOC data (Table 1). The *n*-alkane concentration in the upper-most SP sample is slightly higher (Table 2) than bottom SP sample.

The *n*-alkane distributions are all characterised by strong odd over even chain length preference. The calculated carbon preference index (CPI; Table 3) values of between 6 and 19, in conjunction with the dominance of C₂₄–C₃₃ *n*-alkanes, is consistent with a higher plant origin; specifically the epicuticular waxes of vascular plants (e.g. Eglinton and Hamilton, 1967; Pancost and Boot, 2004).

The relative abundance of the different *n*-alkane homologues varies between the SP and TK sites (Fig. 3). In all but one sample (SP 4, which is characterised by dominant C₃₁ and C₃₃) the most abundant homologues are the C₂₉ and C₃₁. Systematic variation in the dominant homologue can be identified within the SP midden sequence. The normalised C₃₁ index (C₃₁/(C₂₉ + C₃₁)), demonstrates that following an abrupt change at the base of the sequence, C₃₁ is substantially the more abundant homologue in the lower c. 60 mm of the SP midden (Table 3), before progressively decreasing in prominence up sequence. The *n*-alkane distribution in the TK midden is clearly distinct from the SP midden (Fig. 3), showing consistent C₂₉ dominance over C₃₁. Average chain lengths for all three samples from this midden are essentially identical and are consistent with a lower normalised C₃₁ index relative to SP.

4.2. Polar solvent-extractable compounds

A major component of the polar lipid fraction, which is identified in every sample, is benzamide (C₆H₅CONH₂). This compound is the only solvent-extractable nitrogenous compound identified (0.5 $\mu\text{g g}^{-1}$ in the TK midden). A series of *n*-alkanol homologues is clearly detectable, with chain lengths ranging from C₁₆-ol to C₂₈-ol and concentrations slightly lower than the *n*-alkanes. For example, in the TK midden they range between 0.002 and 0.03 $\mu\text{g g}^{-1}$. As is typical of their occurrence in recent sedimentary contexts they display a very strong even over odd chain length preference (e.g. Eglinton and Hamilton, 1967). The dominant homologue in TK (C₂₆-ol) is also typical of a higher plant source (e.g. van Bergen et al., 1997). In the case of SP, the *n*-alkanol distribution is wider, with a broad peak between C₁₆-ol to C₂₀-ol.

The other major compounds in the polar fraction include cholesterol and 5- β -Cholest-5-enol and their hydrogenated products (e.g. cholestanol and 5- β -Cholestanol; 0.8 $\mu\text{g g}^{-1}$). These animal-derived sterols must have originated directly from the hyrax gut content (e.g. Lin and

Table 1

Bulk and acid-treated (TOC) carbon contents and $\delta^{13}\text{C}$ obtained from SP and TK. TOC/TN ratios are also shown for the SP site. Note that Truitjes Kraal samples display no significant change with HCl pre-treatment (labelled "N/A").

Sample code	Sample depth (mm)	Total carbon content (%)	$\delta^{13}\text{C}$ (‰)	TOC (%)	Organic $\delta^{13}\text{C}$ (‰)	TOC/TN
<i>Spitzkoppe</i>						
SP1	15	22.2	−21.6	14.4	−23.5	4.7
SP10	25	24.9	−22.0	18.2	−23.6	6.6
SP2	30	23.1	−20.8	15.1	−23.3	4.3
SP3	40	24.7	−21.6	18.7	−23.0	6.9
SP4	60	25.9	−21.5	18.7	−22.9	8.8
SP5	80	26.6	−21.1	20.1	−21.9	9.3
SP6	90	27.6	−21.1	20.6	−21.9	9.0
SP7	100	25.5	−20.5	19.1	−22.2	8.4
SP9	115	25.9	−20.3	19.8	−22.0	9.1
SP11	120	25.1	−20.2	18.8	−22.1	8.8
<i>Truitjes Kraal</i>						
TK2	20	36.4	−26.9	36.4	N/A	N/A
TK5	30	37.3	−26.2	37.3	N/A	N/A

Table 2

Total concentrations of *n*-alkane homologues for the large samples removed from the SP and TK middens. Original sample masses are included in the bottom row.

<i>n</i> -alkane homologue	SP-top ($\mu\text{g g}^{-1}$)	SP-bottom ($\mu\text{g g}^{-1}$)	TK ($\mu\text{g g}^{-1}$)
21	0.0003	0.0007	0.0013
22	0.0002	0.0006	0.0006
23	0.0013	0.0021	0.0054
24	0.0005	0.0011	0.0017
25	0.0039	0.0065	0.0231
26	0.0008	0.0017	0.0054
27	0.0093	0.0134	0.0946
28	0.0014	0.0017	0.0259
29	0.0213	0.0173	1.1236
30	0.0023	0.0012	0.0588
31	0.0439	0.0191	0.7573
32	0.0021	0.0005	0.0291
33	0.0117	0.0018	0.0702
34	0.0003	0	0
Sample mass (g)	25.533	22.0131	11.9667

Conner, 2001; van Geel et al., 2008). In fact, 5 β -stanols are often used as a means to detect faecal matter inputs to sedimentary or archaeological deposits (e.g. Evershed et al., 1997; Bull et al. 1999). The occurrence of phyto-sterols (e.g. β -Sitosterol c. 0.4 $\mu\text{g g}^{-1}$), which are derived from the structural components of higher plant cell membranes, along with higher plant-derived pentacyclic terpenoids such as α -Amyrin (Volkman et al., 2007) further demonstrates the abundance of plant-derived organic matter in the middens, which must have passed through the animal unaltered by gut microflora.

4.3. Pyrolysis GC/MS

Comparison of the extractable lipid concentrations with the total organic carbon contents clearly indicates that the lipids represent a minor fraction of the total organic matter in hyraceum. Pyrolysis allows an assessment of this (insoluble) macromolecular component via the controlled thermal degradation of a sample followed by the injection of the resulting products into a GC/MS system (e.g. Wampler, 2007). Interpretation of the types and relative proportions of the pyrolysis products provides an indication of the original macromolecular structure and composition. Pyrograms for two representative samples from the SP and TK middens are shown in Fig. 4. The hyraceum pyrolysis products are essentially identical and dominated by aromatic compounds. Some are common in pyrolysates and are not diagnostic, as they may be fragmentation products of a wide range of parent compounds (e.g. styrene; Fig. 4). More interestingly, for both samples the largest (SP) or second largest

Table 3

The characteristics of the *n*-alkane chain length distributions. C_{max} = highest concentration *n*-alkane homologue, ACL = "average chain length" (C₂₃–C₃₃) defined: (C₂₃*23 + C₂₅*25 + C₂₇*27 + C₂₉*29 + C₃₁*31 + C₃₃*33) / (C₂₃ + C₂₅ + C₂₇ + C₂₉ + C₃₁ + C₃₃). CPI = "carbon preference index" (C₂₅–C₃₃) defined: CPI = 0.5 * [(C₂₅ + C₂₇ + C₂₉ + C₃₁ + C₃₃) / (C₂₄ + C₂₆ + C₂₈ + C₃₀ + C₃₂) + (C₂₅ + C₂₇ + C₂₉ + C₃₁ + C₃₃) / (C₂₆ + C₂₈ + C₃₀ + C₃₂ + C₃₄)]. The relative significance of the C₂₉ and C₃₁ homologues is represented by the normalised C₃₁ index: C₃₁ / (C₂₉ + C₃₁).

Sample	Depth (mm)	C _{max}	ACL	C ₃₁ / (C ₃₁ + C ₂₉)	CPI
SP-top	5	31	30.02	0.67	13.08
SP3	40	31	29.66	0.78	6.10
SP4	60	31	31.04	0.89	7.45
SP5	80	31	30.93	0.91	14.65
SP7	100	31	30.54	0.88	8.72
SP9	115	31	30.75	0.91	12.42
SP-bottom	125	31	28.67	0.52	10.6
TK-top	5	29	29.71	0.40	17.23
TK2	20	29	29.83	0.48	11.54
TK5	30	29	29.75	0.38	18.72

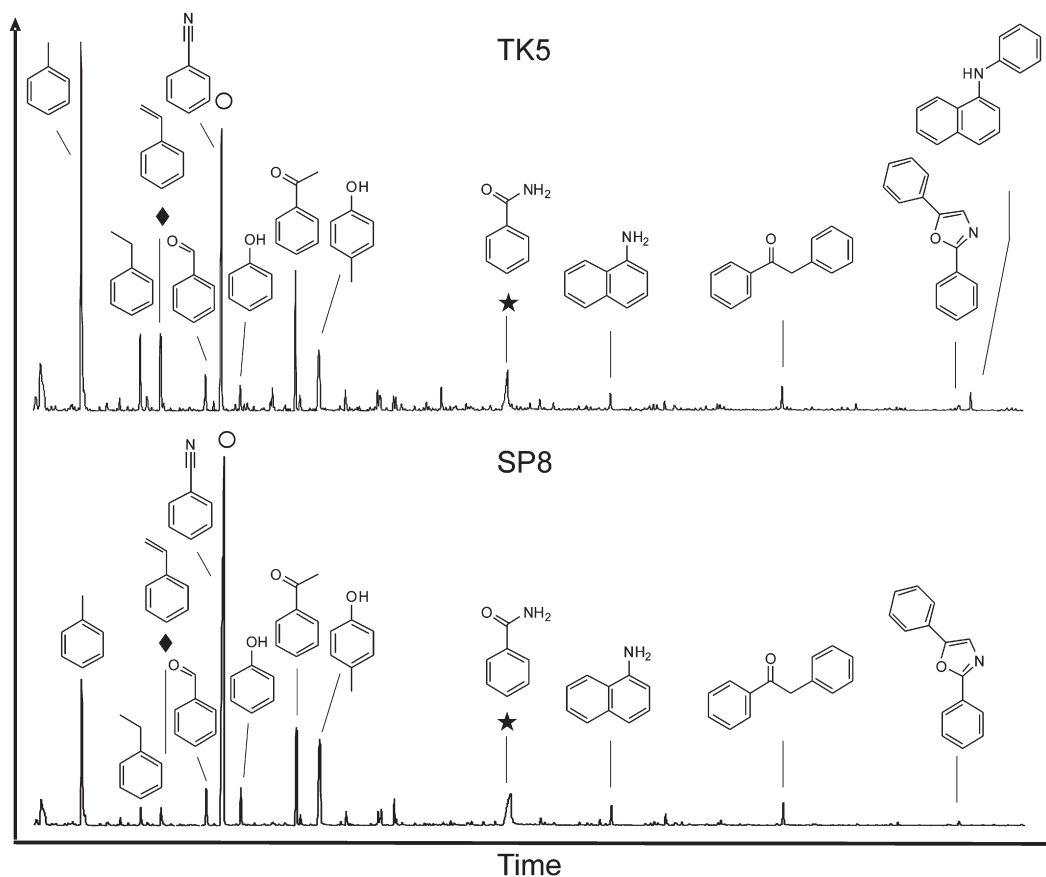


Fig. 4. Pyrograms for the TK (top) and SP (bottom) middens, showing the total ion current (TIC) with no sample pre-treatment. Compounds mentioned in the text are labelled as diamonds (styrene), circles (benzonitrile) and stars (benzamide).

(TK) peak is benzonitrile, which is accompanied by benzamide and additional polyaromatic nitrogen-containing compounds. These are not typical pyrolysis products of plant-derived or sedimentary organic matter, and must be related to animal metabolites.

In both cases, the addition of TMAH reduces the number of pyrolysis products as it prevents the complete fragmentation of the parent molecules. In these samples TMAH results in a shift in the relative significance of the benzonitrile (significantly decreased) and benzamide (increased) (Fig. 5), strongly suggesting that the former is a pyrolysis product of the latter. This, together with the occurrence of more complex polyaromatic nitrogen compounds, suggests that benzamide is likely to be a structural monomer of a larger polymeric structure that forms the organic matrix of the hyraceum. It appears from the solvent extracts that benzamide is also partially soluble. Benzamide and related compounds therefore comprise a significant proportion of the total organic matter within the hyraceum, and are probably the major source of nitrogen as measured in bulk N and $\delta^{15}\text{N}$ measurements. The TOC/N ratio of the hyraceum (Table 1) is akin to that of both benzamide and benzonitrile (7).

Interestingly, common pyrolysis products unequivocally indicative of higher plant inputs, such as lignin monomers, are absent or below detection limits in the pyrolysates. Specific mass traces for lignin pyrolysis products such as guaiacol, syringol and *p*-coumaric acid confirmed this finding. This is however consistent with the lack of observable macro plant remains (cf: pack rat middens; Pearson and Betancourt, 2002, and references therein).

4.4. Compound-specific $\delta^{13}\text{C}$ analysis

Compound specific $\delta^{13}\text{C}$ analyses were conducted on the *n*-alkane lipid extracts from the three large sub-sample extracts. The $\delta^{13}\text{C}$ data

for the most abundant *n*-alkanes are shown in Table 4. The most depleted *n*-alkanes in the SP samples are the C_{29} and C_{31} homologues (Fig. 3), which is consistent with the previous interpretation of a higher plant leaf wax origin. From these data the relative proportions of C_3 and C_4 plant inputs may be estimated using a two component mixing-model (Huang et al., 2000) with C_4 and C_3 end member $\delta^{13}\text{C}$ values of -20% and -35% (Boom et al., 2002), and the weighted (by relative peak area) mean $\delta^{13}\text{C}$. The resulting data imply c. 60% (SP-top) and 50% (SP-bottom) C_4 plant inputs to the SP hyraceum and c. 21% C_4 plant inputs into the TK hyraceum.

The latter result is particularly interesting given that C_4 grasses are virtually absent in the Cederberg today and were probably also absent in the past (e.g. Vogel et al., 1978; Scott and Vogel, 2000). This enrichment of the *n*-alkane $\delta^{13}\text{C}$ may instead reflect a contribution from CAM plants, which are found both in the site vicinity and in the nearby Succulent Karoo Biome (see also Scott and Vogel, 2000). Few studies have reported *n*-alkane $\delta^{13}\text{C}$ data for CAM plants (Collister et al., 1994; Bi et al., 2005; Chikaraishi and Naraoka, 2007), and in each case few species were analysed (none of which were southern African). The data that are available suggest that CAM plant leaf waxes are highly variable, with *n*-alkane $\delta^{13}\text{C}$ values ranging from -21 to -29% (Collister et al., 1994; Bi et al., 2005).

5. Discussion

5.1. The composition of hyraceum

The above analyses demonstrate the presence of both plant and animal-derived organic matter within the middens. The solvent-extractable fraction clearly represents a small proportion of the total organic content of the hyraceum (Tables 1 and 2), and it is only the

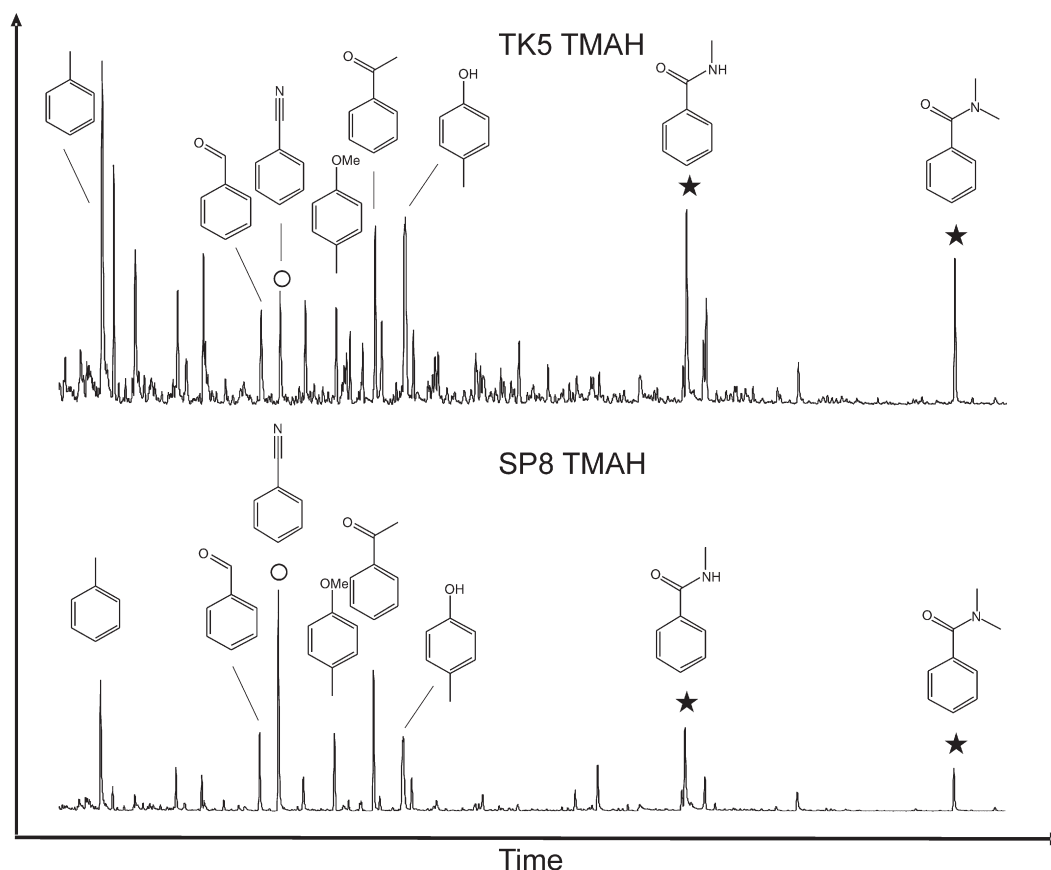


Fig. 5. Example pyrograms (TIC) after the application of TMAH for the TK (top) and SP (bottom) middens. Compounds mentioned in the text are labelled as circles (Benzonitrile) and stars (two methyl derivatives of benzamide, which are a result of the TMAH treatment).

py-GC/MS data that provide a clear indication of the primary nature of the organic matter within hyraceum. The presence of benzamide within the solvent extracts and its great significance within the py-GC/MS data suggests that this compound represents a significant proportion of the hyraceum organic matter. It is possible that benzamide is derived from hippuric acid; a metabolic compound commonly found in the urine of mammals and ruminants (Bristow et al., 1992). Given the dominance of benzamide and related compounds, these are assumed to represent the primary source of nitrogen as determined in bulk stable isotope measurements. Despite visual differences between the middens (Fig. 2), and notable differences in the extractable lipid compositions, these data imply

that bulk $\delta^{15}\text{N}$ data will primarily record the isotopic signature of the same animal-derived metabolic product in both middens.

5.2. Palaeoenvironmental significance

Given the concentration of other lipids and metabolic products within the solvent extracts it seems most plausible to assume that the majority of *n*-alkanes within the hyraceum were derived from the hyraxes' diet. Similarly, van Geel et al (2008) identified plant-derived *n*-alkanes and *n*-alkanols in high concentrations (c. 400 $\mu\text{g g}^{-1}$) within herbivore faeces (mammoth).

The relative abundances of the four major *n*-alkane chain lengths associated with higher plant leaf waxes are plotted in ternary diagrams (Fig. 6) with, for comparison, the southeast Atlantic *n*-alkane data reported by Rommerskirchen et al. (2003). The hyraceum data all plot in broadly the same domains of the diagrams, reflecting the dominance of the C_{29} and C_{31} homologues; with only SP4 showing a significant proportion of C_{33} *n*-alkane (Fig. 6B) and sample SP-bottom (125 mm) exhibiting a relatively larger C_{27} signal (reflected in the lower ACL value for this sample; Table 3 and Fig. 6A). In both diagrams the SP data plot closer to data from marine core sites 5–9, in which terrestrial organic matter was primarily derived from southern African savanna ecosystems (as opposed to sites 1–4). This is consistent with the location of the SP site, although the midden data display greater variability in C_{29} – C_{31} abundance, as well as a stronger dominance of the C_{31} alkane in some cases, compared to the ocean core data. This may reflect some homogenisation of the terrestrial organic matter during transport off the continent (e.g. Eglinton et al., 2002). The TK data clearly plot separately to the SP data, due primarily to the greater significance of the C_{29} *n*-alkane.

Table 4

n-alkane $\delta^{13}\text{C}$ (‰) data for the TK and SP middens. Each mean and accompanying standard deviation is based on 3 separate sample injections. Missing data reflect signals too small for precise peak integration. Weighted mean $\delta^{13}\text{C}$ was determined from C_{27} – C_{31} alkane relative peak areas.

<i>n</i> -alkane homologue	TK $\delta^{13}\text{C}$ (‰)		SP-top $\delta^{13}\text{C}$ (‰)		SP-bottom $\delta^{13}\text{C}$ (‰)	
	Mean	SD	Mean	SD	Mean	SD
25	−29.2	0.6	–	–	−24.5	0.1
27	−30.7	0.3	−25.1	0.5	−24.7	0.1
28	−30.9	0.7	–	–	–	–
29	−32.2	0.5	−27.4	0.3	−28.1	0.1
30	−31.6	0.5	−26.1	0.1	–	–
31	−32.3	0.3	−26.0	0.7	−29.0	0.2
32	−30.6	0.5	−26.7	0.8	–	–
33	−30.7	0.4	−24.8	0.9	−26.7	0.4
Weighted mean	−32.0	–	−25.9	–	−27.5	–

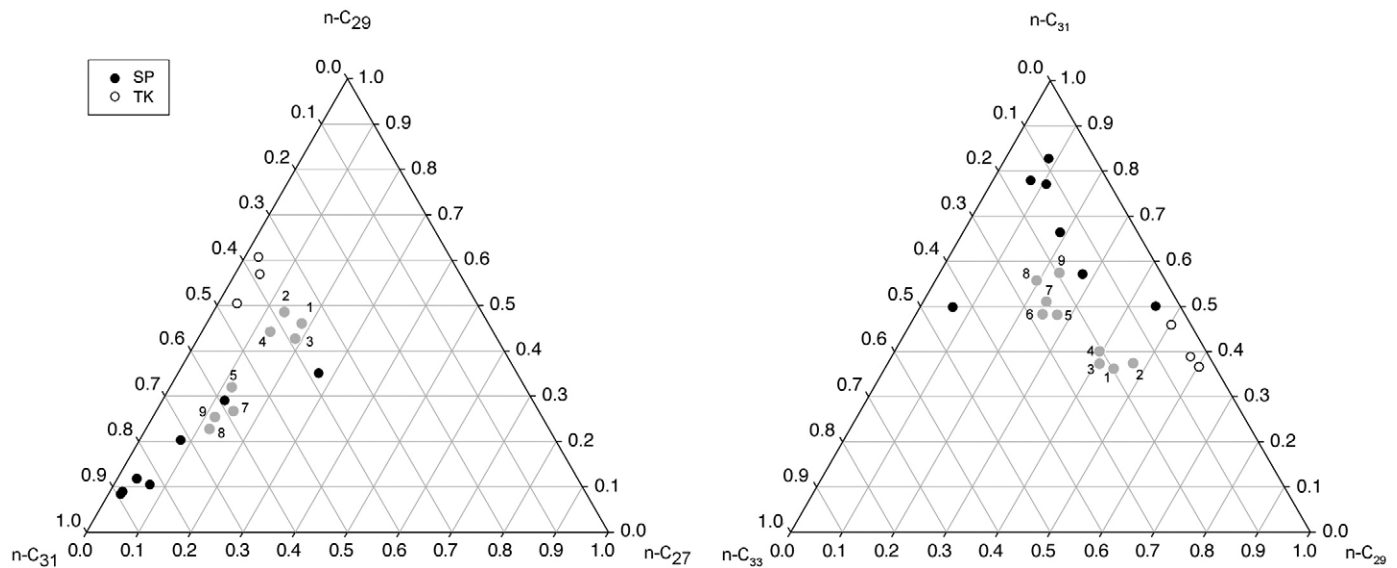


Fig. 6. The relative proportions of C_{27} , C_{28} and C_{29} n -alkane (left) and C_{29} , C_{31} , C_{33} (right) n -alkane homologues extracted from the SP and TK middens plotted in relation to the data of Rommerskirchen et al. (2003) – grey circles. Numbers refer to ocean cores from which these data were derived; running north–south from 1) ODP 1075A; 2) GeoB 1008-3; 3) GeoB1016-3; 4) ODP 1079A; 5) GeoB 1028-5; 6) ODP 1082A; 7) GeoB1710-3; 8) ODP 1084-A; 9) GeoB1722-1.

There is less scatter in the three TK samples, although these subsamples are all comparable in age to one another.

When plotted stratigraphically the normalised C_{31} index for SP midden samples reveals a progressive increase in the relative significance of the C_{29} alkane (Fig. 7). The exact cause of systematic changes in dominant n -alkane chain length within sedimentary archives is still subject to some debate, although large-scale re-organisations in the dominant regional vegetation type (e.g. grasses/herbs versus trees; Schwark et al., 2002; Bai et al., 2008), as well as changes in temperature (Poynter et al., 1989; Castañeda et al., 2009) and/or humidity (Schefuß et al., 2003) have been cited as explanations. In the African context, dust deposits collected from marine transects reveal a strong relationship between n -alkane distribution

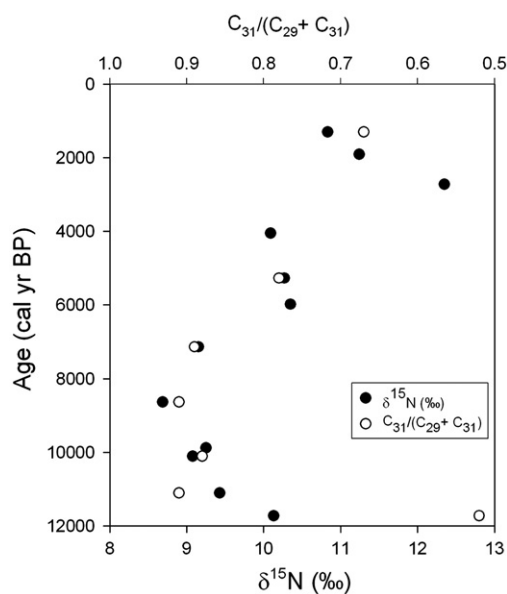


Fig. 7. The $\delta^{15}\text{N}$ and normalised C_{31} index ($C_{31}/(C_{29} + C_{31})$) records plotted stratigraphically. Calibrated radiocarbon ages for the midden SPZ1-3 are shown. Further details of this midden and its chronology are provided in Chase et al. (2009).

and the terrestrial distribution of tropical and savanna vegetation north and south of the equator (Eglinton et al., 2002; Schefuß et al., 2003; Rommerskirchen et al., 2003). Specifically, there is a tendency for the C_{31} n -alkane homologue to become more dominant in organic matter derived from drier savanna regions. This has been associated with a greater occurrence of grasses, and a normalised C_{31} index >0.5 has been interpreted as indicative of predominantly grassy environments (Rommerskirchen et al., 2003; Zhang et al., 2006). The normalised C_{31} index through the SP midden sequence therefore implies a progressive reduction in grass inputs, particularly in the youngest samples (Fig. 7).

The TK midden data are distinct from all of the SP sequence, with notably lower ACLs and normalised C_{31} index values reflecting the dominance of the C_{29} homologue. This result is consistent with the site location in the Western Cape Province, which is characterised by shrubby (primarily C_3) vegetation and a more humid climate than the central Namibian SP site (Rommerskirchen et al., 2003; Schefuß et al., 2003). The compound specific stable isotope data also imply a contribution of CAM plants to the leaf wax lipids at this site. This is cannot be resolved from the homologue distributions (e.g. CPI and C_{max}) given the limited study and variability shown in published examples from CAM plants (e.g. Collister et al., 1994; Bi et al., 2005). This subject has yet to receive systematic study in southern African environments. However, hyraxes have been recorded feeding on succulent plants elsewhere in Africa, despite a preference for fresh grasses when in season, and feeding preferences are usually in proportion to the vegetation present (Hoeck, 1975). Given that pollen from CAM-containing plant families, such as Aizoaceae and Euphorbiaceae is also recorded within the TK midden (Meadows et al., in press), we cannot as yet rule out that CAM plants form a proportion of the Hyrax diet in certain locations, such as the Cederberg and the Succulent Karoo Biome.

The n -alkane $\delta^{13}\text{C}$ data for the SP sequence (-27.5‰ to -25.9‰) are markedly more enriched than the TK midden (-32.0‰), and although limited in number, are also consistent with the inference that greater proportions of C_{31} n -alkanes (higher C_{31} index) tend to correlate with grassier, C_4 -rich vegetation in savanna environments and a more enriched n -alkane $\delta^{13}\text{C}$ (Eglinton et al., 2002; Rommerskirchen et al., 2003). C_4 grasses, notably *Stipagrostis* sp., are very common in the vicinity of Spitzkoppe and northern Namibia (Barnard, 1998; Gil-Romera et al., 2006b), and although some CAM species are

present, midden pollen records from the Huab River region c. 150 km north of SP are dominated by Poaceae and Acanthaceae pollen (Gil-Romera et al., 2006b).

The sampled SP midden sequence spans the period c. 11,600–1300 cal yr BP, within which both the $\delta^{13}\text{C}$ and n -alkane data imply a progressive reduction in the significance of grass-derived organic matter inputs from the mid-late Holocene (Fig. 7). Hoeck (1975) reported that *Procapra johnstoni* tend to favour fresh grass, particularly during the wet season. As grasses became less palatable and/or less abundant during the dry season, the proportion of bushes and trees in the hyrax diet tended to increase (ibid). Brown and Downs (2005) also reported that during the dry season the proportion of tree bark in *Procapra capensis*' diet increased (as grasses dry out). The changing n -alkane composition recorded in the SP midden therefore implies a reduction in the extent of palatable grasses within the local vegetation, and increased feeding on woodier vegetation. Based on the contemporary ecology of this region this shift is suggestive of a period of progressive aridification 6000–2500 cal yr BP, which is consistent with other data from Spitzkoppe. Most notably, the $\delta^{15}\text{N}$ record (Fig. 7), which has been associated with shifts in relative aridity.

6. Conclusions

This initial study demonstrates the good preservation of both plant and animal-derived organic matter within the middens. Plant-derived n -alkanes dominate the apolar lipid fraction, while the polar lipids are dominated by metabolic products from the animal (e.g. cholesterol), plant sterols and n -alkanols. The solvent-extractable fraction represents a small proportion of the total organic matter and the py-GC/MS data provide a first opportunity to consider the macromolecular organic matter composition of hyraceum. The TK and SP middens yield remarkably similar pyrolysates, with the hyraceum dominated by nitrogen-containing aromatic structures. The abundance of benzamide indicates that the majority of this organic matter is derived directly from the hyraxes' urine, which implies that the same-urine-derived-signal probably dominates the measured isotopic ($\delta^{15}\text{N}$) composition of the bulk samples.

The extractable lipid data demonstrate that n -alkane homologue distributions, coupled with the n -alkane $\delta^{13}\text{C}$ pick out differences in the vegetal inputs to middens in ecologically distinct sites, as well as through time in the SP midden sequence. In the case of the SP midden these data record a progressive reduction in grass inputs to the midden, which is commensurate with our understanding of the animal's feeding behaviour and the regional palaeoenvironmental record. This represents a novel approach to reconstructing terrestrial environmental fluctuations in southern African savannas. Given the relative ease by which such homologue distribution data may be acquired, this may prove an extremely valuable tool in unravelling regional palaeoecological dynamics in a region where grasses are frequently over-represented in pollen spectra.

Acknowledgements

Funding for the collection of the middens and radiocarbon ages was variously provided by the Leverhulme Trust, the South African National Research Foundation and the University of Cape Town Research Committee. We thank the University of Leicester for support of the stable isotope facility in the Department of Geography. The reviewers are thanked for their helpful comments.

References

Bai, Y., Fang, X.M., Nie, J.S., Wang, Y.L., Wu, F.L., 2008. A preliminary reconstruction of the paleoecological and paleoclimatic history of the Chinese Loess Plateau from the application of biomarkers. *Palaeogeography, Palaeoclimatology, Palaeoecology* 271, 161–169.

Barnard, P., 1998. Biological Diversity in Namibia: Windhoek, Namibian National Biodiversity Task Force. Directorate of Environmental Affairs. 332 pp.

Bi, X., Sheng, G., Lui, X., Li, C., Fu, J., 2005. Molecular and carbon and hydrogen isotopic composition of n -alkanes in plant leaf waxes. *Organic Geochemistry* 36, 1405–1417.

Boom, A., Marchant, R., Hoogheemstra, H., Sinninghe-Damste, J.S., 2002. CO_2 and temperature-controlled altitudinal shifts of C_4 and C_3 dominated grasslands allow reconstruction of palaeoatmospheric $p\text{CO}_2$. *Palaeogeography, Palaeoclimatology, Palaeoecology* 177, 151–168.

Bristow, A.W., Whitehead, D.C., Cockburn, J.E., 1992. Nitrogenous constituents in the urine of cattle, sheep and goats. *Journal of the Science of Food and Agriculture* 59, 387–394.

Brown, K.J., Downs, C.T., 2005. Seasonal behavioural patterns of free-living rock hyrax (*Procapra capensis*). *Journal of the Zoological Society of London* 265, 311–326.

Bull, I.D., Simpson, I.A., Dockrill, S.J., Evershed, R.P., 1999. Organic geochemical evidence for the origin of ancient anthropogenic soil deposits at Tofts Ness, Sanday, Orkney. *Organic Geochemistry* 30, 535–556.

Castañeda, I.S., Werne, J.P., Johnson, T.C., Filley, T.R., 2009. Late Quaternary vegetation history of southeast Africa: the molecular isotope record from Lake Malawi. *Palaeogeography, Palaeoclimatology, Palaeoecology* 275, 100–112.

Chase, B.M., Meadows, M.E., 2007. Late Quaternary dynamics of southern Africa's winter rainfall zone. *Earth Science Reviews* 84, 103–138.

Chase, B.M., Meadows, M.E., Scott, L., Thomas, D.S.G., Marais, E., Sealy, J., Reimer, P.J., 2009. A record of rapid Holocene climate change preserved in hyrax middens from southwestern Africa. *Geology* 37, 703–706.

Chikaraishi, Y., Naraoka, H., 2007. $\delta^{13}\text{C}$ and δD relationships among three n -alkyl compound classes (n -alkanoic acid, n -alkane, and n -alkanol) of terrestrial higher plants. *Organic Geochemistry* 38, 198–215.

Codron, D., Codron, J., Lee-Thorp, J.A., Sponheimer, M., de Ruiter, D., Sealy, J., Grant, R., Fourie, N., 2007. Diets of savanna ungulates from stable carbon isotope composition of faeces. *Journal of Zoology* 273, 21–29.

Collister, J.W., Rieley, G., Stern, B., Eglinton, G., Fry, B., 1994. Compound-specific $\delta^{13}\text{C}$ analyses of leaf lipids from plants with differing carbon dioxide metabolisms. *Organic Geochemistry* 21, 619–627.

Conte, M.H., Weber, J.C., 2002. Plant biomarkers in aerosols record isotopic discrimination of terrestrial photosynthesis. *Nature* 417, 639–641.

Cowling, R.M., Hilton-Taylor, C., 1999. Plant biogeography, endemism and diversity. In: Dean, W., Milton, S. (Eds.), *The Karoo: Ecological Patterns and Processes*. Cambridge University Press, Cambridge.

Eglinton, G., Hamilton, R., 1967. Leaf epicuticular waxes. *Science* 156, 1322–1335.

Eglinton, T.I., Eglinton, G., Dupont, L., Sholkovitz, E.R., Montluçon, D., Reddy, C.M., 2002. Composition, age, and provenance of organic matter in NW African dust over the Atlantic Ocean. *Geochemistry, Geophysics, Geosystems* 3 (8). doi:10.1029/2001GC000269.

Evershed, R.P., Bethell, P.H., Reynolds, P., Walsh, N.J., 1997. 5 β -stigmastanol and related 5 β -stanols as biomarkers of manuring: analysis of modern experimental materials and assessment of the archaeological potential. *Journal of Archaeological Science* 24, 485–495.

Farquhar, G.D., Ehleringer, J.R., Hubick, K.T., 1989. Carbon isotope discrimination and photosynthesis. *Annual Review of Plant Physiology and Plant Molecular Biology* 40, 503–537.

Gibbs-Russell, G.E., Watson, L., Koekemoer, M., Smook, L., Baker, N.P., Anderson, H.M., Dallwitz, M.J., 1990. Grasses of southern Africa. *Memoirs of the Botanical Survey of South Africa*, vol. 58. Government Printer, Pretoria. 437 pp.

Gil-Romera, G., Scott, L., Marais, E., Brook, G.A., 2006a. Late Holocene environmental change in the northwestern Namib Desert margin: new fossil pollen evidence from hyrax middens. *Palaeogeography, Palaeoclimatology, Palaeoecology* 249, 1–17.

Gil-Romera, G., Scott, L., Marais, E., Brook, G.A., 2006b. Middle- to late-Holocene moisture changes in the desert of northwest Namibia derived from fossil hyrax dung pollen. *Holocene* 16, 1073–1084.

Hijmans, R., Cameron, S.E., Parra, J.L., Jones, P.G., Jarvis, A., 2005. Very high resolution interpolated climate surfaces for global land areas. *International Journal of Climatology* 25, 1965–1978.

Hoeck, H.N., 1975. Differential feeding behaviour of the sympatric Hyrax *Procapra johnstoni* and *Heterohyrax brucei*. *Oecologia* 22, 15–47.

Hollocher, T.C., Chin, K., Hollocher, K.T., Kruge, M.A., 2001. Bacterial residues in coprolite of herbivorous dinosaurs: role of bacteria in mineralization of feces. *Paleosols* 16, 547–565.

Huang, Y., Dupont, L., Sarnthein, M., Hayes, J.M., Eglinton, G., 2000. Mapping of C_4 plant input from North West Africa into North East Atlantic sediments. *Geochimica et Cosmochimica Acta* 64, 3505–3513.

Lin, D.S., Conner, W.E., 2001. Faecal steroids of the coprolite of a Greenland Eskimo mummy, AD 1475: a clue to dietary sterol intake. *American Journal of Clinical Nutrition* 74, 44–49.

Linder, H.P., 2003. The radiation of the Cape flora, southern Africa. *Biological Reviews of the Cambridge Philosophical Society* 78, 597–638.

Meadows, M.E., Seliane, M., and Chase, B.M. (in press). Holocene palaeoenvironments of the Cederberg and Swartuggens mountains, Western Cape, South Africa: pollen and stable isotope evidence from hyrax dung middens. *Journal of Arid Environments*. doi:10.1016/j.jaridenv.2009.04.020.

Pancost, R.D., Boot, C.S., 2004. The palaeoclimatic utility of terrestrial biomarkers in marine sediments. *Marine Chemistry* 92, 239–261.

Pearson, S., Betancourt, J.L., 2002. Understanding arid environments using fossil rodent middens. *Journal of Arid Environments* 50, 499–511.

Poynter, J.G., Farrimond, P., Brassell, S.C., Eglinton, G., 1989. Aeolian-derived higher-plant lipids in the marine sedimentary record: Links with paleoclimate. In: Leinen, M., Sarnthein, M. (Eds.), *Palaeoclimatology and Palaeometeorology: Modern and Past Patterns of Global Atmosphere Transport*. Kluwer, pp. 435–462.

- Prinsloo, L.C., 2007. Rock hyraxes: a cause of San rock art deterioration? *Journal of Raman Spectroscopy* 38, 496–503.
- Rommerskirchen, F., Eglinton, G., Dupont, L., Güntner, U., Wenzel, C., Rullkötter, J., 2003. A north to south transect of Holocene southeast Atlantic continental margin sediments: relationship between aerosol transport and compound-specific $\delta^{13}\text{C}$ plant biomarker and pollen records. *Geochemistry, Geophysics, Geosystems* 4 (12), 1101.
- Rommerskirchen, F., Eglinton, G., Dupont, L., Rullkötter, J., 2006. Glacial/interglacial changes in southern Africa: compound-specific $\delta^{13}\text{C}$ land plant biomarker and pollen records from southeast Atlantic continental margin sediments. *Geochemistry, Geophysics, Geosystems* 7, Q08010.
- Rundel, P.W., Esler, K.J., Cowling, R.M., 1999. Ecology and phylogenetic patterns of carbon isotope discrimination in the winter-rainfall flora of the Richtersveld, South Africa. *Plant Ecology* 142, 133–148.
- Sale, J.B. 1965. Some aspects of the behaviour and ecology of the rock hyraxes (*Genus Procavia* and *Heterohyrax*) in Kenya. Unpublished PhD thesis, University of London.
- Schefuß, E., Rathmeyer, V., Stuut, J.-B.W., Jansen, J.H.F., Sinninghe-Damsté, J.S., 2003. Carbon isotope analyses of *n*-alkanes in dust from the lower atmosphere over the central eastern Atlantic. *Geochimica et Cosmochimica Acta* 67, 1757–1767.
- Schulze, R.E., 1997. Atlas of Agro-Hydrology & Agro-Climatology. WRC Report TT82/96. Water Resource Commission, Pretoria.
- Schulze, E.D., Ellise, R., Schulze, W., Timborn, P., 1996. Diversity, metabolic types and $\delta^{13}\text{C}$ carbon isotope ratios in the grass flora of Namibia in relation to growth form, precipitation and habitat conditions. *Oecologia* 106, 352–369.
- Schwark, L., Zink, K., Lechterbeck, J., 2002. Reconstruction of postglacial to early Holocene vegetation history in terrestrial Central Europe via cuticular lipid biomarkers and pollen records from lake sediments. *Geology* 30, 463–466.
- Scott, L., 1996. Palynology of hyrax middens: 2000 years of palaeoenvironmental history in Namibia. *Quaternary International* 33, 73–79.
- Scott, L., Bousman, C.B., 1990. Palynological analysis of hyrax middens from southern Africa. *Palaeogeography, Palaeoclimatology, Palaeoecology* 76, 367–379.
- Scott, L., Vogel, J.C., 2000. Evidence for environmental conditions during the last 20,000 years in southern Africa from ^{13}C in fossil hyrax dung. *Global and Planetary Change* 26, 207–215.
- Scott, L., Woodborne, S., 2007. Pollen analysis and dating of Late Quaternary faecal deposits (hyraceum) in the Cederberg, Western Cape, South Africa. *Review of Palaeobotany and Palynology* 144, 123–134.
- Scott, L., Marais, E., Brook, G.A., 2004. Fossil hyrax dung and evidence of Late Pleistocene and Holocene vegetation types in the Namib Desert. *Journal of Quaternary Science* 19, 829–832.
- van Bergen, P.F., Bull, I.D., Poulton, P.R., Evershed, R.P., 1997. Organic geochemical studies of soils from the Rothamsted Classical Experiments I. Total lipids, solvent insoluble residues and humic acids from Broadbalk Wilderness. *Organic Geochemistry* 26, 117–135.
- van Geel, B., Aptroot, A., Baittinger, C., Birks, H.H., Bull, I.D., Cross, H.B., Evershed, R.P., Gravendeel, B., Kompanje, E.J.O., Kuperus, P., Mol, D., Nierop, K.G.J., Pals, J.P., Tikhonov, A.N., van Reenen, G., van Tienderen, P.H., 2008. The ecological implications of a Yakutian mammoth's last meal. *Quaternary Research* 69, 361–376.
- Vogel, J.C., Fuls, A., Ellis, R.P., 1978. The geographical distribution of Kranz grasses in South Africa. *South African Journal of Science* 74, 209–215.
- Volkman, J.K., Revill, A.T., Bonham, P.I., Clementson, L.A., 2007. Sources of organic matter in sediments from the Ord River in tropical northern Australia. *Organic Geochemistry* 38, 1039–1060.
- Wampler, T.P., 2007. Applied pyrolysis: an overview. In: Wampler, T.P. (Ed.), *Applied Pyrolysis Handbook*. CRC press. Taylor and Francis, Boca Raton, pp. 1–26.
- Zhang, Z., Zhao, M., Eglinton, G., Lu, H., Huang, C.Y., 2006. Leaf wax lipids as paleovegetational and paleoenvironmental proxies for the Chinese Loess Plateau over the last 170 kyr. *Quaternary Science Reviews* 25, 575–594.